Oxidation-State-Dependent Reactivity and Catalytic Properties of a Rh(I) Complex Formed from a Redox-Switchable Hemilabile Ligand

Caroline S. Slone,[†] Chad A. Mirkin,*[,†] Glenn P. A. Yap,[‡] Ilia A. Guzei,[‡] and Arnold L. Rheingold[‡]

Contribution from the Department of Chemistry, 2145 Sheridan Road, Northwestern University, Evanston, Illinois 60208, and Department of Chemistry and Biochemistry, University of Delaware, Newark, Delaware 19716

Received July 14, 1997[⊗]

Abstract: The synthesis and characterization of a phosphinoalkylarene, redox-switchable hemilabile ligand (RHL), (η^5-C_5H_5)Fe(η^5-$C_5H_4C_6H_4OCH_2CH_2PPh_2$) (**1**), are reported. This ligand, which incorporates a redox-active ferrocenyl group, exhibits oxidation-state-dependent bonding properties and, hence, affords electrochemical control over the electronic and steric environments of bound transition metal centers. Two equivalents of **1** complex to Rh(I) to yield a bis(phosphine), η^6-arene complex [(η^1:η^6-(η^5-C_5H_5)Fe(η^5-$C_5H_4C_6H_4OCH_2CH_2PPh_2$))($\eta^1$-($\eta^5$-$C_5H_5$)Fe($\eta^5$-$C_5H_4C_6H_4OCH_2CH_2PPh_2$))Rh]$^+BF_4^-$ (**2**). Single-crystal X-ray diffraction studies of **2**·1.25CH_2Cl_2, as well as solution spectroscopic data of **2**, are consistent with this formulated piano-stool geometry. Foremost, the properties of **2** as a function of bound RHL state-of-charge are extensively investigated. Interestingly, 2D ^{1}H NMR exchange spectroscopy (EXSY) studies demonstrate significantly faster intramolecular η^6-arene, free arene exchange rates only upon oxidation of the ligand chelated to the Rh(I) center, as found in $\mathbf{2}^{2+}$. This faster exchange rate was used as a qualitative measure of the increased lability of the η^6-aryl group upon RHL oxidation. Moreover, activation parameters measured for the arene−arene exchange reaction of $\mathbf{2}^{2+}$ also support a decrease in the Rh(I)−arene interaction only upon oxidation of the ferrocenyl group on the bound η^6-arene moiety. In addition, changes in the stoichiometric and catalytic reactivity of **2** upon RHL oxidation are consistent with the observed charge-dependent arene−arene exchange behavior. Significantly, labilization of a weakly bound η^6-arene moiety in $\mathbf{2}^{2+}$ results in substantial increases in both the acetonitrile bonding affinity and allyl ethyl ether isomerization activity of the Rh(I)−RHL complex. In contrast, no significant changes in the reactivity of **2** were observed upon oxidation of the ligand which contained the ferrocenylarene not bound to the Rh(I) center, as found in $\mathbf{2}^{+}$. This dependence of complex reactivity on RHL oxidation state demonstrates the utility of such novel metal complexes for the reversible, electrochemical control of transition metal center small molecule uptake or catalytic activity via the selective labilization of weakly coordinating groups upon ligand oxidation.

Introduction

Strategies for controlling transition metal center reactivity have relied on the synthetic manipulation of either the steric or the electronic properties of bound ligands.[1−3] Studies of ligands which impose steric constraints on reactive transition metal centers have demonstrated that a metal steric environment can greatly affect small molecule bonding properties[1] and catalytic activity.[2] Furthermore, tuning of the electron-donating or the electron-withdrawing properties of ligands also has been shown to impact the electronic nature of a transition metal complex and, therefore, its reactivity.[3] Traditionally, such modulation of transition metal complex reactivity has focused on changes in the ligand's properties before being bound to a metal center. Recently, however, electrochemical methods have been used to control the properties of metal complexes through the use of redox switchable hemilabile ligands (RHLs).[4−8]

The ligand reported herein, (η^5-C_5H_5)Fe(η^5-$C_5H_4C_6H_4OCH_2$-CH_2PPh_2) (**1**), is one of an extensive series of RHLs studied in our group which afford electrochemical control over both the steric and electronic environments of bound transition metal

* Author to whom correspondence should be addressed.
[†] Northwestern University.
[‡] University of Delaware.
[⊗] Abstract published in *Advance ACS Abstracts,* October 15, 1997.

(1) (a) Gladysz, J. A.; Boone, B. J. *Angew. Chem., Int. Ed. Engl.* **1997**, *36*, 550. (b) Boone, B. J.; Klein, D. P.; Seyler, J. W.; Méndez, N. Q.; Arif, A. M.; Gladysz, J. A. *J. Am. Chem. Soc.* **1996**, *118*, 2411. (c) Fernandez, A. L.; Prock, A.; Giering, W. P. *Organometallics* **1996**, *15*, 2784. (d) Beckett, R. P.; Burgess, V. A.; Davies, S. G.; Krippner, G. Y.; Sutton, K. H.; Whittaker, M. *Inorg. Chim. Acta* **1996**, *251*, 265. (e) Mizutani, T.; Ema, T.; Tomita, T.; Kuroda, Y.; Ogoshi, H. *J. Am. Chem. Soc.* **1994**, *116*, 4240. (f) Collman, J. P.; Zhang, X.; Wong, K.; Brauman, J. I. *J. Am. Chem. Soc.* **1994**, *116*, 6245.

(2) (a) Abbenhuis, H. C. L.; Burckhardt, U.; Gramlich, V.; Martelletti, A.; Spencer, J.; Steiner, I.; Togni, A. *Organometallics* **1996**, *15*, 1614. (b) Togni, A.; Burckhardt, U.; Gramlich, V.; Pregosin, P. S.; Salzmann, R. *J. Am. Chem. Soc.* **1996**, *118*, 1031. (c) Lindner, E.; Fisahn, P.; Fawzi, R.; Steimann, M. *Chem. Ber.* **1996**, *129*, 191. (d) van Rooy, A.; Kamer, P. C. J.; van Leeuwen, P. W. N. M.; Goubitz, K.; Fraanje, J.; Veldman, N.; Spek, A. L. *Organometallics* **1996**, *15*, 835. (e) Myers, A. W.; Jones, W. D. *Organometallics* **1996**, *15*, 2905. (f) Kotha, S.; *Tetrahedron* **1994**, *50*, 3639. (g) Burk, M. J.; Feaster, J. E.; Nugent, W. A.; Harlow, R. L. *J. Am. Chem. Soc.* **1993**, *115*, 10125. (h) Noyori, R. *Science* **1990**, *248*, 1194. (i) Whitesell, J. K. *Chem. Rev.* **1989**, *89*, 1581. (j) Chan, A. S. C.; Pluth, J. J.; Halpern, J. *Inorg. Chim. Acta* **1979**, *37*, L477.

(3) (a) Schnyder, A.; Hintermann, L.; Togni, A. *Angew. Chem., Int. Ed. Engl.* **1995**, *34*, 931. (b) RajanBabu, T. V.; Ayers, T. A.; Casalnuovo, A. L *J. Am. Chem. Soc.* **1994**, *116*, 4101. (c) Casalnuovo, A. L.; RajanBabu, T. V.; Ayers, T. A.; Warren, T. H. *J. Am. Chem. Soc.* **1994**, *116*, 9869. (d) RajanBabu, T. V.; Ayers, T. A. *Tetrahedron Lett.* **1994**, *35*, 4295. (e) Chang, S.; Heid, R. M.; Jacobsen, E. N. *Tetrahedron Lett.* **1994**, *35*, 669. (f) Hawkins, J. M.; Loren, S.; Nambu, M. *J. Am. Chem. Soc.* **1994**, *116*, 1657. (g) Nishiyama, H.; Yamaguchi, S.; Kondo, M.; Itoh, K. *J. Org. Chem.* **1992**, *57*, 4306. (h) Haltermann, R. L.; McEvoy, M. A. *J. Am. Chem. Soc.* **1992**, *114*, 980. (i) Jacobsen, E. N.; Zhang, W.; Güler, M. L. *J. Am. Chem. Soc.* **1991**, *113*, 6703. (j) Baldy, C. J.; Morrison, D. L.; Elliott, C. M. *Langmuir* **1991**, *7*, 2376. (k) Schrock, R. R.; DePue, R. T.; Feldman, J.; Schaverien, C. J.; Dewan, J. C.; Liu, A. H. *J. Am. Chem. Soc.* **1988**, *110*, 1423.

S0002-7863(97)02360-3 CCC: $14.00

centers.[4] These ligands have a substitutionally inert group and a substitutionally labile one. When bound to a transition metal center, such as Rh(I), the bonding affinity of the substitutionally labile moiety of the RHL can be controlled by adjusting the oxidation state of a redox group that is covalently attached to it, eq 1. Furthermore, it has been shown that the magnitude of this effect can be tailored by altering the RHL phosphine substituents,[4a] varying the weak bonding group (e.g. ether,[4a,c−d] thioether,[4a] η^6-arene,[4b] etc.), or controlling the distance between the redox-active group and the transition metal center.[4a]

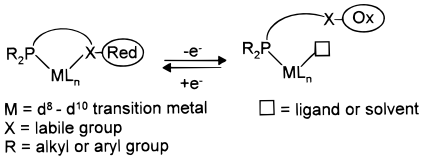

(1)

Both metal-based and ligand-based strategies have been used to alter the properties of metal complexes electrochemically. For instance, systems which incorporate redox-active groups into macrocyclic ligands, such as crown ethers, thiocrowns, and cryptands, have been used to electrochemically control macrocycle bonding constants for metal ions.[5,6] Although the majority of such redox-active sequestering agents have been designed to complex alkali and alkaline earth cations,[5] a number of macrocycles which target late transition metal ions also have been investigated.[6] These systems, however, are not desirable for the reversible modulation of transition metal center reactivity since oxidation of the redox-active ligand can result in expulsion of the metal center of interest. Complementary to the modulation of ligand bonding via ligand oxidation are metal-based strategies which focus on changes in the electronic properties of the metal center itself.[7,8] For example, many have shown that oxidation or reduction of a metal center can change the bonding strength or hapticity of a bound ligand.[7] Kochi and co-workers, for instance, have shown that reduction of (η^5-C_5H_4-Me)$Mn(CO)_2$(NCMe) labilizes a bound acetonitrile ligand toward substitution reactions.[7a] In contrast to this metal-based strategy, others have used *substitutionally inert* redox-active ligands to affect the electronic properties of bound transition metals without oxidation of the metal center itself.[8] Wrighton and co-workers, for example, have demonstrated that oxidation of the cobaltocene group in [(1,1′-bis(diphenylphosphino)-cobaltocene)$Re(CO)_4$]PF_6 increases the rate of nucleophilic attack of N_3^- at a CO ligand by a factor of 5400[8a] and that cobaltocene oxidation affects the rates of catalytic reactions mediated by a 1,1′-bis(diphenylphosphino)cobaltocene Rh(I) complex.[8b] Since a substitutionally inert redox-active ligand was used, however, this strategy only yielded electrochemical modulation of transition metal electronic properties and not a selective opening and closing of coordination sites at the metal center as with the RHL approach.

Past work in our group has illustrated the utility of RHL complexes for the reversible electrochemical control over both the electronic and steric properties of bound transition metal centers.[4] In this report, we demonstrate how changes in the properties of a phosphinoalkylarene RHL complex, [(η^1:η^6-(η^5-C_5H_5)Fe(η^5-$C_5H_4C_6H_4OCH_2CH_2PPh_2$))($\eta^1$-($\eta^5$-$C_5H_5$)Fe($\eta^5$-$C_5H_4C_6H_4OCH_2CH_2PPh_2$))Rh]$^+BF_4^-$ (**2**), upon ligand oxidation result in substantial differences in complex reactivity. Specifically, we address how the thermodynamic perturbation in complex free energy that occurs upon RHL oxidation directly translates into changes in complex stoichiometric and catalytic reactivity. Therefore, by selectively labilizing weakly bound η^6-arene moieties in the Rh(I)−RHL complex **2**, we have been able to demonstrate for the first time that the small molecule bonding properties and the catalytic activity of that complex can be substantially affected simply upon ligand oxidation.

Results

Synthesis, Characterization, and Solid-State Structure of 2. The synthesis of **1** and its complexation to Rh(I) to form the 18-electron, bis(phosphine), η^6-arene piano-stool complex (**2**) was reported in a preliminary communication.[4b] RHL **1** was synthesized by the reaction of ferrocenylphenol[9] and $ClCH_2$-CH_2Cl in distilled H_2O at reflux for 15 h in the presence of excess KOH and a catalytic amount of $^nBu_4NI$ to form (η^5-C_5H_5)Fe(η^5-$C_5H_4C_6H_4OCH_2CH_2Cl$) in 46% yield, eq 2. The reaction of (η^5-C_5H_5)Fe(η^5-$C_5H_4C_6H_4OCH_2CH_2Cl$) with $KPPh_2$ in THF at 0 °C gave ligand **1** in 80% yield, eq 2. Ligand **1** and

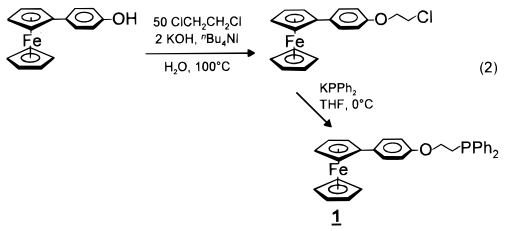

(2)

1

its precursor were fully characterized by ^{1}H NMR spectroscopy, ^{31}P NMR spectroscopy, electron ionization (EI) mass spectrometry, and elemental analysis.

(4) (a) Allgeier, A. M.; Slone, C. S.; Mirkin, C. A.; Liable-Sands, L. M.; Yap, G. P. A.; Rheingold, A. L. *J. Am. Chem. Soc.* **1997**, *119*, 550. (b) Sassano, C. A.; Mirkin, C. A. *J. Am. Chem. Soc.* **1995**, *117*, 11379. (c) Singewald, E. T.; Mirkin, C. A.; Stern, C. L. *Angew. Chem., Int. Ed. Engl.* **1995**, *34*, 1624. (d) Allgeier, A. M.; Singewald, E. T.; Mirkin, C. A.; Stern, C. L. *Organometallics* **1994**, *13*, 2928.

(5) (a) Beer, P. D.; Chen, Z.; Grieve, A.; Haggitt, J. *J. Chem. Soc., Chem. Commun*. **1994**, 2413. (b) Beer, P. D. *Endeavour* **1992**, *16*, 182. (c) Beer, P. D.; Tite, E. L.; Ibbotson, A. *J. Chem. Soc., Dalton Trans.* **1991**, 1691. (d) Medina, J. C.; Goodnow, T. T.; Rojas, M. T.; Atwood, J. L.; Lynn, B. C.; Kaifer, A. E.; Gokel, G. W. *J. Am. Chem. Soc*. **1992**, *114*, 10583. (e) Chen, Z.; Gokel, G. W.; Echegoyen, L. *J. Org. Chem.* **1991**, *56*, 3369. (f) Beer, P. D.; Keefe, A. D.; Sikanyika, H.; Blackburn, C.; McAleer, J. F. *J. Chem. Soc., Dalton Trans*. **1990**, 3289. (g) Andrews, M. P.; Blackburn, C.; McAleer, J. F.; Patel, V. D. *J. Chem. Soc., Chem. Commun*. **1987**, 1122.

(6) (a) Beer, P. D.; Nation, J. E.; Harman, M. E.; Hursthouse, M. B. *J. Organomet. Chem*. **1992**, *441*, 465. (b) Tendero, M. J. L.; Benito, A.; Martínez-Máñez, R.; Soto, J.; Payà, J.; Edwards, A. J.; Raithby, P. R. *J. Chem. Soc., Dalton Trans.* **1996**, 343. (c) Sato, M.; Suzuki, K.; Asano, H.; Sekino, M.; Kawata, Y.; Habata, Y.; Akabori, S. *J. Organomet. Chem*. **1994**, *470*, 263. (d) Sato, M.; Shigeta, H.; Sekino, M.; Akabori, S. *J. Organomet. Chem*. **1993**, *458*, 199. (e) Sato, M.; Tanaka, S.; Akabori, S.; Habata, Y. *Bull. Chem. Soc. Jpn*. **1986**, *59*, 1515. (f) De Santis, G.; Fabbrizzi, L.; Licchelli, M.; Pallavicini, P.; Perotti, A. *J. Chem. Soc., Dalton Trans.* **1992**, 3283.

(7) For transition metal oxidation-state-dependent ligand bonding strength see the following: (a) Hershberger, J. W.; Kochi, J. K. *J. Chem. Soc., Chem. Commun*. **1982**, 212. (b) Kuchynka, D. J.; Amatore, C.; Kochi, J. K. *Inorg. Chem.* **1986**, *25*, 4087. (c) Hecht, M.; Schultz, F. A.; Speiser, B. *Inorg. Chem.* **1996**, *35*, 5555. (d) Yeung, L. K., Kim, J. E.; Chung, Y. K.; Rieger, P. H.; Sweigart, D. A. *Organometallics* **1996**, *15*, 3891. For transition metal oxidation-state-dependent ligand hapticity, see the following: (e) Connelly, N. G.; Emslie, D. J. H.; Metz, B.; Orpen, A. G.; Quayle, M. J. *J. Chem. Soc., Chem. Commun.* **1996**, 2289. (f) Bowyer, W. J.; Geiger, W. E. *J. Am. Chem. Soc.* **1985**, *107*, 5657. (g) Harman, W. D.; Sekine, M.; Taube, H. *J. Am. Chem. Soc*. **1988**, *110*, 2439. (h) Kuchynka, D. J.; Kochi, J. K. *Inorg. Chem.* **1988**, *27*, 2574.

(8) (a) Lorkovic, I. M.; Wrighton, M. S.; Davis, W. M. *J. Am. Chem. Soc.* **1994**, *116*, 6220. (b) Lorkovic, I. M.; Duff, R. R., Jr.; Wrighton, M. S. *J. Am. Chem. Soc.* **1995**, *117*, 3617. (c) Kotz, J. C.; Nivert, C. L. *J. Organomet. Chem*. **1973**, *52*, 387. (d) Kotz, J. C.; Nivert, C. L.; Lieber, J. M.; Reed, R. C. *J. Organomet. Chem.* **1975**, *91*, 87. (e) Elschenbroich, C.; Stohler, F. *Angew. Chem., Int. Ed. Engl.* **1975**, *14*, 174.

(9) Weinmayr, V. *J. Am. Chem. Soc*. **1955**, *77*, 3012.

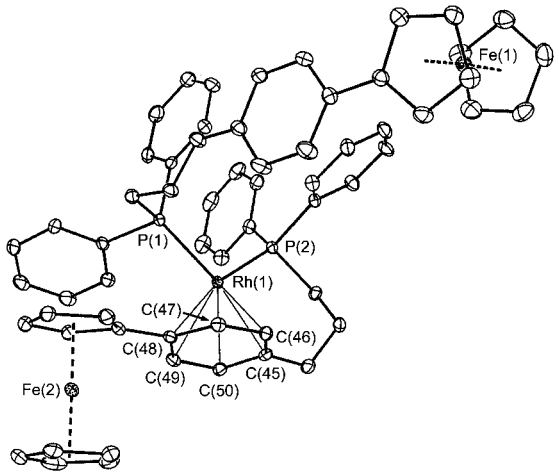

Figure 1. ORTEP diagram of cation **2**·1.25CH_2Cl_2. Thermal ellipsoids are drawn a 30% probability.

The Rh(I) piano-stool complex **2** was synthesized by the reaction of $[RhCl(COT)_2]_2$[10] (COT = cyclooctene) with 2 equiv of $AgBF_4$ in CH_2Cl_2, followed by dilution and reaction of the resulting solution with 4 equiv of **1** at −78 °C, eq 3. Pure samples of **2** were fully characterized by ^{1}H NMR spectroscopy, ^{31}P NMR spectroscopy, high-resolution fast atom bombardment (FAB^+) mass spectrometry, and a single-crystal X-ray diffraction study.

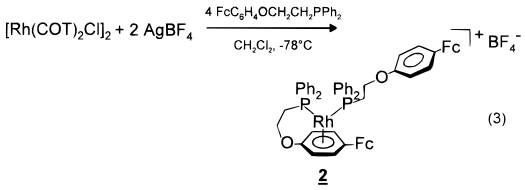

2

Single-crystals of **2**·1.25CH_2Cl_2 suitable for X-ray diffraction were grown from the the slow diffusion of pentane into a CH_2Cl_2 solution of **2**. Two crystallographically independent, but chemically equivalent, ion pairs were located in the asymmetric unit. An ORTEP diagram of one of the two cations is shown in Figure 1, and crystallographic data are presented in Table 1. Selected bond distances and angles are given for both crystallographically independent cations in Table 2. The observed Rh−C bond distances are in the expected range for monomeric Rh(I) compounds with a bis(phosphine), η^6-arene piano-stool geometry (Rh−C = 2.217−2.516 Å), whereas the monodentate Rh−P bond distances are slightly longer than literature values (Rh−P = 2.217−2.251 Å).[11] The structure of **2**·1.25CH_2Cl_2 also compares well with that of an analogous compound, [(η^1:η^6-$C_6H_5OCH_2CH_2PPh_2$)(η^1-$C_6H_5OCH_2CH_2PPh_2$)Rh]$^+BF_4^-$ (**3**), previously reported by our group, Chart 1.[12] In particular, both independent cations are similar to **3** in that they possess a Rh−P bond distance for the chelating phosphine ligand which is shorter (2.2457(8) and 2.2393(8) Å) than the Rh−P bond distance for the monodentate phosphine ligand (2.2827(9) and 2.2771(9) Å).

Table 1. Crystallographic Data for **2**·1.25CH_2Cl_2

formula	$C_{61.25}H_{56.50}BCl_{2.5}F_4Fe_2O_2P_2Rh$
formula weight	1276.55
crystal system	triclinic
space group	$P\bar{1}$
a, Å	15.9857(2)
b, Å	19.2497(2)
c, Å	19.77310(10)
α, deg	70.9728(4)
β, deg	88.8718(7)
γ, deg	77.3017(1)
V, Å^3	5602.53(10)
Z	4
crystal color, habit	orange, block
D(calc), g cm^{-3}	1.513
μ(Mo Kα), cm^{-1}	10.35
temp, K	173(2)
size, mm^3	0.30 × 0.30 × 0.20
diffractometer	Siemens P4/CCD
radiation	Mo Kα (*λ* = 0.710 73 Å)
R(*F*), %[a]	4.10
R(w*F*^{2}) %[a]	12.60

[a] Quantity minimized: $R(wF^2) = \sum[w(F_o^2 - F_c^2)^2/\sum[w(F_o^2)^2]^{1/2}$; $R = \sum\Delta/\sum\Delta(F_o)$, $\Delta = |(F_o - F_c)|$.

Table 2. Selected Distances (Å) and Angles (deg) of **2**·1.25CH_2Cl_2

Rh(1)−P(1)	2.2827(8)	Rh(2)−P(1′)	2.2771(9)
Rh(1)−P(2)	2.2457(8)	Rh(2)−P(2′)	2.2393(9)
Rh(1)−C(45)	2.302(3)	Rh(2)−C(45′)	2.303(3)
Rh(1)−C(46)	2.345(3)	Rh(2)−C(46′)	2.339(3)
Rh(1)−C(47)	2.383(3)	Rh(2)−C(47′)	2.375(3)
Rh(1)−C(48)	2.358(3)	Rh(2)−C(48′)	2.371(3)
Rh(1)−C(49)	2.360(3)	Rh(2)−C(49′)	2.372(3)
Rh(1)−C(50)	2.366(3)	Rh(2)−C(50′)	2.357(3)
Rh(1)−arene centroid	1.877(3)	Rh(2)−arene centroid	1.877(3)
P(1)−Rh(1)−P(2)	96.38(3)	P(1′)−Rh(2)−P(2′)	96.07(3)
C(45)−C(46)−C(47)	120.0(3)	C(45′)−C(46′)−C(47′)	119.7(3)
C(46)−C(47)−C(48)	119.9(3)	C(46′)−C(47′)−C(48′)	120.2(3)
C(47)−C(48)−C(49)	119.2(3)	C(47′)−C(48′)−C(49′)	119.6(3)
C(48)−C(49)−C(50)	121.2(3)	C(48′)−C(49′)−C(50′)	120.2(3)
C(49)−C(50)−C(45)	118.9(3)	C(49′)−C(50′)−C(45′)	118.9(3)
C(50)−C(45)−C(46)	120.8(3)	C(50′)−C(45′)−C(46′)	120.8(3)

Chart 1

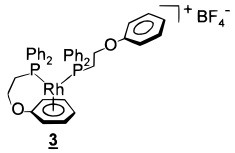

3

Similar to **3**, the bound arene ligand in **2**·1.25CH_2Cl_2 shows small deviations from planarity; the average deviation for the two independent cations is 0.02 (Å). This is 4 times the deviations from planarity for the phosphorus-bound phenyl rings. Through extensive theoretical calculations done by other researchers, it has been shown that arenes bound to transition metal centers, such as Rh(I), adopt boat conformations as a result of the interaction between a metal d-orbital and an η^6-arene π-orbital.[13] Indeed, several complexes which are isoelectronic with **2**, such as **3**, have been reported to contain arene ligands with such deformations from planarity.[11−13] However, unlike the boat conformation observed for **3**, only the bond between the Rh center and the C atom connected to the chelate arm is significantly shorter than the other Rh−C bonds in **2**·1.25CH_2Cl_2. Perhaps, the attachment of the ferrocenyl moiety to the aryl group creates unfavorable steric interactions which prevent the formation of a boat conformation as observed for **3**. This

(10) Porri, L.; Lionetti, A.; Allegra, G.; Immirzi, A. *Chem. Commun.* **1965**, 336.

(11) (a) Singewald, E. T. ; Slone, C. S.; Stern, C. L.; Mirkin, C. A.; Yap, G. P. A.; Liable-Sands, L. M.; Rheingold, A. L. *J. Am. Chem. Soc.* **1997**, *119*, 3048. (b) Alvarez, M.; Lugan, N.; Donnadieu, B.; Mathieu, R. *Organometallics* **1995**, *14*, 365. (c) Westcott, S. A.; Taylor, N. J.; Marder, T. B.; Baker, R. T.; Jones, N. J.; Calabrese, J. C. *J. Chem. Soc., Chem. Commun.* **1991**, 304. (d) Townsend, J. M.; Blount, J. F. *Inorg. Chem.* **1981**, *20*, 269. (e) Albano, P.; Aresta, M.; Manassero, M. *Inorg Chem.* **1980**, *19*, 1069.

(12) Singewald, E. T.; Shi, X.; Mirkin, C. A.; Shofer, S. J.; Stern, C. L. *Organometallics* **1996**, *15*, 3062.

(13) Muetterties, E. L.; Bleeke, J. R.; Wucherer, E. J.; Albright, T. A. *Chem. Rev.* **1982**, *82*, 499.

steric interaction also is reflected in the longer Rh−arene centroid distances for **2**·1.25CH_2Cl_2 (1.877(3) Å for both independent cations) as compared with the Rh−arene centroid distance in **3** (1.840(3) Å). Also, the structure of the ferrocenyl moieties in both independent cations of **2**·1.25CH_2Cl_2 are similar to analogous aromatic substituted ferrocenes studied by other workers in that the angles between the planes of the substituted cyclopentadienyl and aryl rings are relatively small (angles between the planes range from 13.3° to 19.3°).[14]

Compound **2** also has been spectroscopically characterized, and all solution data are consistent with its solid-state structure. The ^{31}P NMR spectrum of **2** exhibits two resonances at δ 34.9 and δ 31.3 which are assigned to magnetically and chemically inequivalent P atoms due to the coupling to each other and the ^{103}Rh nucleus. Each resonance appears as a doublet of doublets (J_{Rh-P} = 204.4 and 209.7 Hz; J_{P-P} = 39.3 Hz) with coupling constants that are in the expected region for Rh(I) complexes with this type of geometry.[11,12] Also, all resonances in the ^{1}H NMR spectrum of **2** have been assigned either by comparison with the spectrum of the free ligand **1** or by a ^{1}H COSY NMR experiment.

Synthesis and Characterization of 2^+ and 2^{2+}. To explore the effects of oxidation of the redox-active ferrocenyl groups in **2** on its reactivity, the oxidized forms (2^+ and 2^{2+}) were synthesized and isolated. The mixed-valence complex 2^+ and the doubly-oxidized complex 2^{2+} were formed by the reaction of **2** with either 1 or 2 equiv of $AgBF_4$, respectively, in CH_2Cl_2 at room temperature, eqs 4 and 5. Complexes 2^+ and 2^{2+} were isolated from the resulting Ag^0 mirrors in extremely high yields and characterized by ^{1}H NMR and ^{31}P NMR spectroscopy.

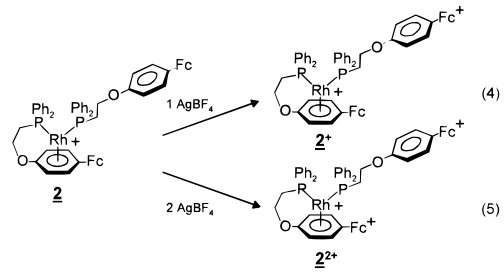

Although the oxidation reactions resulted in complexes with paramagnetic ferrocenium centers, which are known to cause large contact and dipolar shifts and line broadening,[15] NMR spectroscopy was still a useful characterization tool. The resonances in the ^{31}P NMR spectra, in particular, were very well resolved since the ^{31}P nuclei in 2^+ and 2^{2+} are far from the ferrocenium centers and, therefore, have little interaction with the unpaired electron spin density. The changes in the ^{31}P NMR spectrum of **2** upon sequential oxidation were small, but highly reproducible, Figure 2. Upon the addition of 1 equiv of $AgBF_4$ to **2**, the ^{31}P NMR resonances at δ 34.9 and 31.3 shifted upfield to δ 34.3 and 30.3, respectively. From a ^{31}P-{^{1}H}−^{1}H HETCOR experiment of compound **3**, we conclude that those resonances in the ^{31}P NMR spectrum which are the most upfield correspond to the P atom in the monodentate ligand on Rh(I).[12] Thus, upon oxidation of **2** to 2^+, the chemical shift of the ^{31}P NMR resonance of the monodentate phosphine ligand changed the most ($\Delta\delta_{mono}$ = 1.0 and $\Delta\delta_{chel}$ = 0.6). This

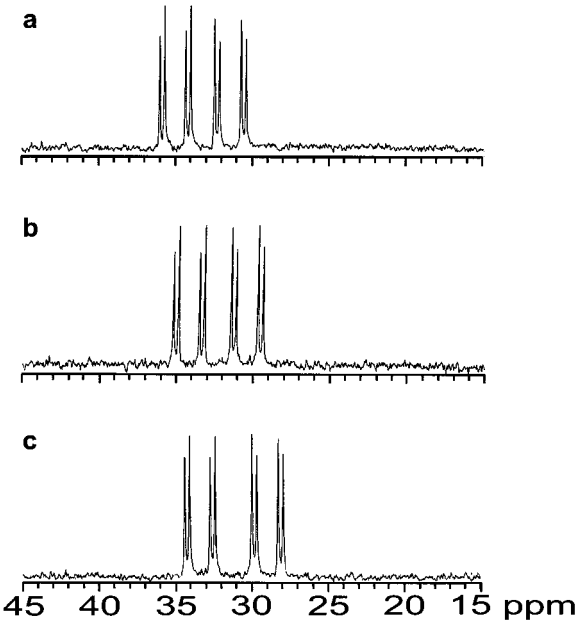

Figure 2. The ^{31}P NMR spectra in CD_2Cl_2 of all oxidation states (a) before the addition of oxidant (**2**), (b) after the addition 1 equiv of $AgBF_4$ (2^+), and (c) after the addition of 2 equiv of $AgBF_4$ (2^{2+}).

observation indicates that the mixed-valence form (2^+) contains a ferrocenium group in the monodentate, and not the chelated phosphine ligand, respectively. Note, the cyclic voltammetry of **2** in CH_2Cl_2 shows the ferrocenyl group on the unbound arene ligand to be 143 mV easier to oxidize than the ferrocenyl group on the arene bound to the cationic Rh(I) center (vida infra). Upon the addition of a second equivalent of $AgBF_4$, the ^{31}P NMR resonances for the chelated and the monodentate phosphine ligands shifted even more upfield to δ 33.4 and 29.0, respectively. Therefore, the observed changes in the ^{31}P NMR spectra of these complexes easily identify ligand oxidation state and Rh(I)−RHL complex purity.

Unlike the ^{31}P NMR spectra of 2^+ and 2^{2+}, the assignment of the resonances in the corresponding ^{1}H NMR spectra was not straightforward. Many resonances were broad and experienced large shifts upon ligand oxidation and changes in complex concentration. However, a comparison of the 1D spectra and an examination of the ^{1}H COSY spectra of **2**, 2^+, and 2^{2+} at the same concentration and temperature (0.024 M in CD_2Cl_2 at 20 °C) afforded assignment of all resonances in these complexes. In particular, the methylene resonances α to the phosphine groups (CH_2PPh_2) were characteristic of ligand oxidation state. For instance, upon the formation of 2^+, the multiplet corresponding to the α protons of the monodentate phosphine ligand shift from δ 2.06 to 1.79, while the position of the quartet corresponding to the α protons in the chelated ligand shift from δ 1.71 to 0.95. Furthermore, these methylene resonances in 2^{2+} are observed at δ 1.53 and 0.27 for the monodentate and chelated phosphine ligands, respectively.

NMR Kinetic Studies. Previously, it was determined that complex **2** undergoes a degenerate intramolecular, free arene, η^6-arene exchange reaction.[4b] In this study, the rate of this unique exchange reaction was utilized as a measure of the relative lability of the η^6-arene ligand on the Rh(I) center in all states-of-charge of **2** (Scheme 1). The rates of the exchange process for the reduced (**2**), mixed-valence (2^+), and doubly-oxidized (2^{2+}) forms were determined by ^{1}H NMR 2D exchange spectroscopy (EXSY) experiments. In general, EXSY is an extremely useful technique for detecting dynamic processes with rates of 10^2-10^{-2} s^{-1}.[16]

(14) (a) Beer, P. D.; Sikanyika, H.; Blackburn, C.; McAleer, J. F.; Drew, M. G. B. *J. Chem. Soc., Dalton Trans.* **1990**, 3295. (b) Loubser, C.; Imrie, C.; van Rooyen, P. H. *Adv. Mater.* **1993**, *5*, 45. (c) Allen, F. H.; Trotter, J.; Williston, C. S. *J. Chem. Soc. A* **1970**, 907.

(15) (a) Sharp, R. R. In *Nuclear Magnetic Resonance*: Webb, G. A., Ed.; The Chemical Society: London, 1994; Vol. 24, p 469. (b) Materikova, R. B.; Babin, V. N.; Solodovnikov, S. P.; Lyatifov, I. R.; Petrovsky, P. V.; Fedin, E. I. Z. *Naturforsch.* **1980**, *35b*, 1415.

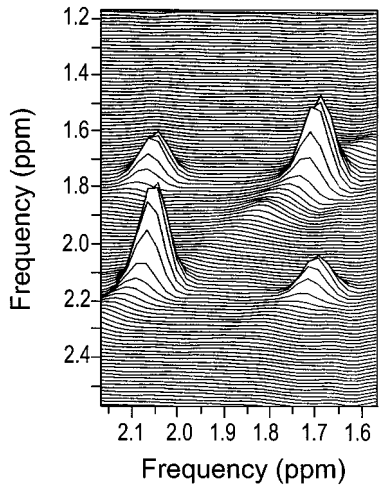

Figure 3. The CH_2PPh_2 region of the ^{1}H NMR EXSY spectrum of **2** in CD_2Cl_2 at 30 °C with $t_m = 0.5$ s.

Scheme 1

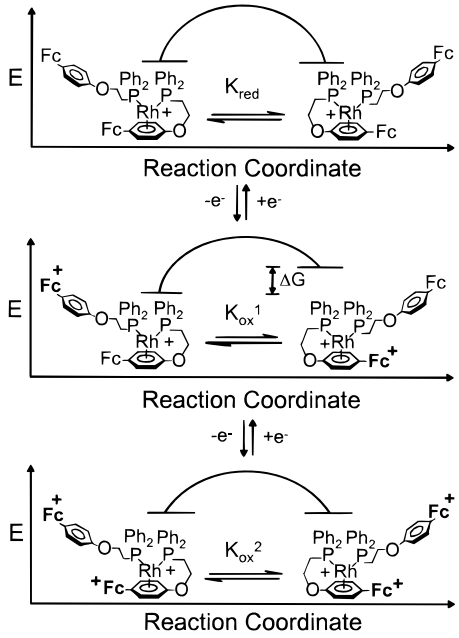

Since the ^{1}H NMR CH_2PPh_2 resonances of the RHL are diagnostic of ligand oxidation state, these resonances were monitored in the 2D EXSY experiments. A ^{1}H EXSY spectrum of **2** is shown in Figure 3. In this plot, the one-dimensional NMR spectrum corresponding to the resonances of the α-methylene protons in the chelated and monodentate phosphine ligands is plotted along the diagonal, and the observed cross peaks are indicative of those protons undergoing chemical exchange. The rates of the exchange reaction were determined by obtaining the volumes of the diagonal and cross peaks for each complex and relating them to the mixing time (see the Experimental Section).[16] The measured rates of the intramolecular arene-arene exchange reaction (Scheme 1) at 20 °C are given in Table 3. These exchange rates demonstrate an increased lability of the η^6-arene ligand in the doubly oxidized complex $\mathbf{2}^{2+}$ ($k = 0.51 \pm 0.04$ s^{-1}) as compared to the labilities of the bound arenes in the reduced complex **2** and the mixed-valence complex $\mathbf{2}^+$ ($k = 0.36 \pm 0.02$ s^{-1} and $k = 0.33 \pm 0.03$ s^{-1}, respectively).[17]

In addition, rate measurements over a range of temperatures gave the activation parameters for the exchange process from the Eyring equation.[18] The Eyring plots obtained for **2**, $\mathbf{2}^+$, and $\mathbf{2}^{2+}$ are shown in Figure 4, and the activation parameters are given in Table 3. From these data, it can be seen that $\Delta G^{\ddagger}_{(293)}$ for this process does not vary considerably; however, the activation parameters, $\Delta H^{\ddagger}$ and $\Delta S^{\ddagger}$, for **2**, $\mathbf{2}^+$, and $\mathbf{2}^{2+}$ exhibit experimentally significant variations. For example, the $\Delta H^{\ddagger}$ of exchange is less for the doubly oxidized complex ($\mathbf{2}^{2+}$) than for both the reduced (**2**) and the mixed-valence ($\mathbf{2}^+$) complexes; these values for **2** and $\mathbf{2}^+$ are the same within experimental error. Moreover, the $\Delta S^{\ddagger}$ of exchange for $\mathbf{2}^{2+}$ is of a different sign than the $\Delta S^{\ddagger}$ values for both **2** and $\mathbf{2}^+$.

Table 3. Rates and Activation Parameters for the Arene−Arene Exchange Reaction

complex	k (s^{-1})[a]	$\Delta G^{\ddagger}_{(293)}$ (kcal/mol)[b]	$\Delta H^{\ddagger}$ (kcal/mol)[b]	$\Delta S^{\ddagger}$ (cal/mol K)[b]
2	0.36 ± 0.02	$+17.50 \pm 0.05$	$+22 \pm 2$	$+15 \pm 5$
$\mathbf{2}^+$	0.33 ± 0.03	$+17.55 \pm 0.05$	$+20 \pm 2$	$+9 \pm 5$
$\mathbf{2}^{2+}$	0.51 ± 0.04	$+17.29 \pm 0.06$	$+13 \pm 2$	-15 ± 7

[a] Arene−arene exchange rate at 20 °C. [b] Activation parameters from Eyring plots.

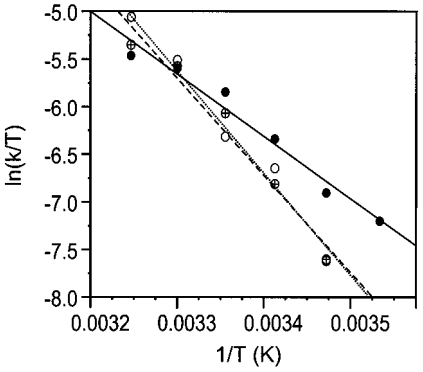

Figure 4. Eyring plots for all oxidation states: (open circle) reduced complex, **2**; (crossed circle) mixed-valance complex, $\mathbf{2}^+$; (filled circle) double oxidized complex, $\mathbf{2}^{2+}$.

Quantification of the Thermodynamic Perturbation of 2 upon RHL Oxidation. The cyclic voltammogram of **2** in CH_2Cl_2/0.1 M ^{n}BuNPF$_6$ exhibits three reversible waves (Figure 5a). The first wave is assigned to the Fe^{II}/Fe^{III} couple of the ferrocenyl group on the unbound arene since the $E_{1/2}$ value of −30 mV vs FcH/FcH$^+$ is identical, within experimental error, to that of the free ligand ($E_{1/2} = -27$ mV) under similar conditions. The second wave at $E_{1/2} = +113$ mV vs FcH/FcH$^+$ corresponds to the oxidation of the ferrocenyl group attached to the bound arene ligand and the wave at $E_{1/2} = +630$ mV vs FcH/FcH$^+$ is assigned to a Rh^I/Rh^{II} couple based on previous work done in our group.[12] In fact, the latter oxidation is an internal diagnostic marker that implies no unusual rearrangement by the complex upon ferrocenyl oxidation. The piano-stool geometry of **2** is one of the few geometries which stabilize Rh(II) with these types of ligands.[12]

From the cyclic voltammogram of **2**, it was possible to quantitate the effects of ligand oxidation. For systems that involve more than two oxidation states, ladder diagrams relating reactants and products through chemical and electron transfer processes can be used in conjunction with $E_{1/2}$ values to obtain important thermodynamic information. The ladder diagram

(16) Perrin, C. L.; Dwyer, T. J. *Chem. Rev.* **1990**, *90*, 935.

(17) For the arene−arene exchange reaction for $\mathbf{2}^+$, a subsequent fast electron transfer step most likely occurs after the rate determining step. Since this fast step is thermodynamically favorable, the values for k, $\Delta G^{\ddagger}$, $\Delta H^{\ddagger}$, and $\Delta S^{\ddagger}$ are a measure for the step in which the ferrocenyl arene is displaced from the Rh(I) center.

(18) Sandström, J. *Dynamic NMR Spectroscopy*; Academic Press: London, 1982.

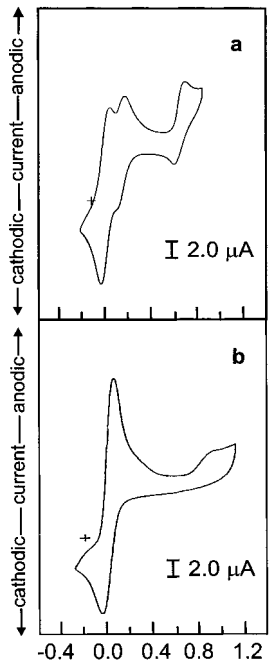

Figure 5. Cyclic voltammetry of **2** measured at 20 mV/s at a glassy carbon electrode (8.0×10^{-5} cm^2): (a) in CH_2Cl_2/0.1 M $^nBu_4NPF_6$ and (b) in 1% CH_3CN in CH_2Cl_2/0.1 M $^nBu_4NPF_6$.

Scheme 2

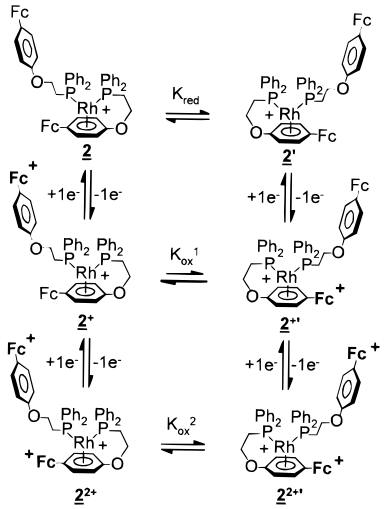

shown in Scheme 2 relates arene−arene exchange equilibria to the electrochemical reactions involving ligand oxidation. Using the Nernst equation, a relationship between the arene−arene exchange equilibria of **2** and one of its oxidized forms ($\mathbf{2}^+$) was derived: $\Delta E_{1/2} = -(RT/nF)\ln(K_{ox}^1/K_{red})$.[19] Significantly, since K_{red} is the equilibrium constant for a degenerate reaction, and therefore equal to 1, it is possible to directly calculate K_{ox}^1 if the $E_{1/2}$ values for the electrochemical reactions going from **2** to $\mathbf{2}^+$ and **2′** to $\mathbf{2}^{+\prime}$ are measurable. Even though the $E_{1/2}$ for the latter process is not experimentally obtainable, it can be assumed to be the same as the $E_{1/2}$ for the process going from $\mathbf{2}^+$ to $\mathbf{2}^{2+}$. This is a reasonable assumption since the electronic communication between the ferrocenyl group attached to the free arene and the formally charged Rh(I) center is negligible. Indeed, the $E_{1/2}$ of ferrocenyl group attached to the free arene in complex **2** is virtually identical to that of the uncomplexed ligand **1**. Furthermore, because of the distance between the two ferrocenyl groups in **2**, electronic communication between them also is assumed to be negligible (e.g. the electronic communication between the two ferrocenyl groups in 1,2-diferrocenyltetramethylethane can not be measured by electrochemical methods; the ethoxy−Rh−arene spacer in **2** is much longer than a tetramethylethyl spacer).[20]

The two ferrocenyl-based waves in the cyclic voltammogram in Figure 5a were better resolved using differential pulse voltammetry. The measured $\Delta E_{1/2}$ of 143 mV corresponded well to the cyclic voltammetry data, and was used to calculate a K_{ox}^1 of 3.8×10^{-3} and a ΔG of 3.3 kcal/mol at 20 °C, Schemes 1 and 2. The change in free energy (ΔG) is the thermodynamic perturbation of the complex that results from RHL ligand oxidation and could be termed the thermodynamic "RHL effect". Therefore, by simply changing the oxidation state of **2**, we have been able to destabilize the metal complex by 3.3 kcal/mol. Presumably, the majority of this effect is associated with a decrease in Rh(I)−arene bond strength upon RHL oxidation. It is also important to note that the change in free energy of the metal complex upon replacing the ferrocenylarene ligand with an arene moiety containing a ferrocenium group can only be measured from a single cyclic voltammogram when intramolecular degenerate exchange reactions are possible. In contrast, the absolute thermodynamic perturbation that results from ligand oxidation cannot be obtained if only nondegenerate processes are possible. In the latter case, cyclic voltammetry merely yields a ratio of equilibrium constants for the reactions involving the oxidized and reduced species.

Ligand Oxidation-State-Dependent Acetonitrile Bonding. In the reduced state, complex **2** reacts with acetonitrile at room temperature to form a mixture of the square-planar, *cis*- and *trans*-bis(acetonitrile) adducts, **4** and **5**, in a ratio of 3:1, eq 6. The ^{31}P NMR spectrum of **4** and **5** exhibits resonances at δ 35.9 and 22.2, respectively. Each resonance appears as a doublet with J_{Rh-P} values of 174.8 Hz for the *cis* adduct and 131.7 Hz for the *trans* adduct. The reactivity of **2** toward acetonitrile was similar to the reactivity of the analogous complex 3.[12] Interestingly, when **2** was reacted with acetonitrile

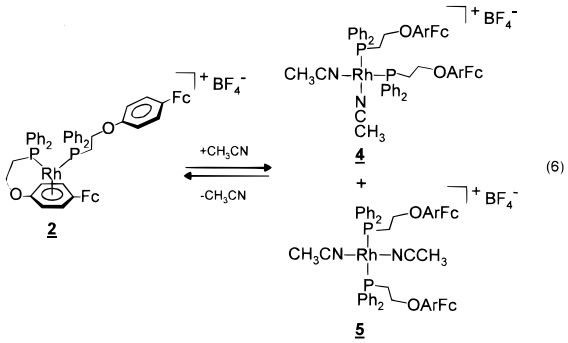

(6)

at low temperature (−78 °C), the *cis* adduct **4** was formed exclusively. As the temperature was then raised to 25 °C, the *cis* adduct slowly converted to the *trans* adduct **5** until a 3:1 *cis* to *trans* ratio was obtained. At 25 °C, the observed *cis* to *trans* ratio of 3:1 corresponds to a $\Delta G_{(298)}$ of −0.65 kcal/mol for the reaction going from **5** to **4**. Furthermore, upon removal of acetonitrile (48 h exposure to vacuum), both **4** and **5** were completely converted back to complex **2**.

Another way to quantify the "RHL effect" is to compare the equilibria between **2** and its acetonitrile adducts **4** and **5** before and after oxidation of the ligand chelated to the metal center. If the Rh(I)−arene bond is indeed weakened upon oxidation of a pendant redox-active ferrocenyl group, then the Rh(I) center's

(19) Bard, A. J.; Faulkner, L. R. *Electrochemical Methods*; John Wiley & Sons: New York, 1980.

(20) Morrison, W. H., Jr.; Krogsrud, S.; Hendrickson, D. N. *Inorg. Chem.* **1973**, *12*, 1998.

Scheme 3

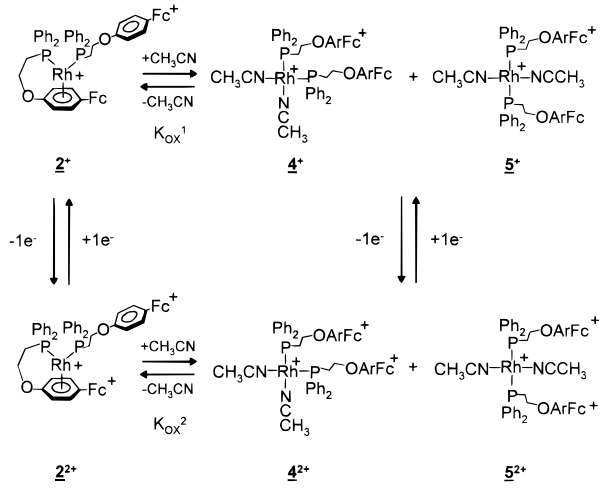

bonding affinity for small molecules such as CH_3CN would be expected to increase upon oxidation. To determine if this was the case, the electrochemical behavior of **2** in the presence of CH3CN was studied, Figure 5b. The cyclic voltammetry of **2** in CH_2Cl_2/0.1 M ^{n}BuNPF$_6$ is markedly different from **2** in 1% CH_3CN in CH_2Cl_2/0.1 M nBuNPF6. Upon the addition of CH_3CN to the electrochemical cell, the three waves that were observed for **2** in CH_2Cl_2/0.1 M ^{n}BuNPF$_6$ disappear. Instead, a single wave with an $E_{1/2}$ value of -20 mV vs FcH/FcH$^+$ is observed. This oxidation potential is consistent with the displacement of the η^6-arene ligand in **2** by CH_3CN, as was observed via NMR spectroscopy, and the simultaneous oxidation of both free ferrocenyl groups. In addition, the well-defined, reversible Rh^{I}/Rh^{II} couple at $+630$ mV vs FcH/FcH$^+$ was replaced by a broad, irreversible wave with an E_{pa} value of $+992$ mV vs FcH/FcH$^+$. This electrochemical irreversibility is common for 16-electron, square-planar Rh(I) complexes with coordination environments similar to those found in **4** and **5**.[4a]

The difference in $E_{1/2}$ values associated with the oxidation of the ligand chelated to the Rh(I) center and the oxidation of the same ligand after CH_3CN displacement, $\Delta E_{1/2}$, can be used to estimate the ratio of equilibrium constants for the displacement of a ferrocenium, η^6-arene ligand compared to the displacement of the more electron rich ferrocenyl, η^6-arene ligand by CH_3CN (K_{ox}^2/K_{ox}^1), Scheme 3. Using the Nernst equation, which relates the equilibria involving $\mathbf{2}^+$, $\mathbf{4}^+$, and $\mathbf{5}^+$ to those involving $\mathbf{2}^{2+}$, $\mathbf{4}^{2+}$, and $\mathbf{5}^{2+}$, a relationship between $\Delta E_{1/2}$ and K_{ox}^2/K_{ox}^1 was derived; $\Delta E_{1/2} = -(RT/nF)\ln(K_{ox}^2/K_{ox}^1)$.[19] For the reactions depicted in the square-wave diagram shown in Scheme 3, the measured $\Delta E_{1/2}$ value of 133 mV corresponds to a K_{ox}^2/K_{ox}^1 ratio of 1.8×10^2. Since the $E_{1/2}$ values for **2** and its CH_3CN adducts were measured in CH_2Cl_2/0.1 M ^{n}BuNPF$_6$ and 1% CH_3CN in CH_2Cl_2/0.1 M ^{n}BuNPF$_6$, respectively, any solvent effects on half-wave potentials were assumed to be negligable.

Ligand Oxidation-State-Dependent Isomerization Studies. Another way to assess the change in the properties of the transition metal center upon ligand oxidation is to monitor the catalytic activity of complex **2** as a function of the ligand's state-of-charge. To demonstrate that RHL oxidation can significantly affect the reactivity of an RHL complex, we chose a well-understood catalytic transformation for Rh(I) transition metal centers, the isomerization of allyl substrates.[21] The reaction in eq 7 was chosen because it is known that bis(phosphine)Rh(I) complexes isomerize such allyl substrates.[21a] Herein, catalyst

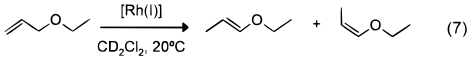

(7)

concentrations were kept constant and substrate-to-Rh catalyst ratios of either 10:1 or 100:1 were used. In order to quantify the extent to which oxidation of the ligand bound to the Rh(I) center affected its catalytic activity, the isomerization activties for **2**, $\mathbf{2}^+$, and $\mathbf{2}^{2+}$ were investigated. For the runs using the mixed-valence ($\mathbf{2}^+$) and doubly oxidized complexes ($\mathbf{2}^{2+}$), the catalyst was generated prior to each experiment and ^{1}H and ^{31}P NMR spectroscopy were utilized to confirm complete and clean oxidation reactions. The concentrations of the products (*cis*- and *trans*-ethyl 1-propenyl ether) were followed by ^{1}H NMR spectroscopy, and the transition metal catalyst was monitored by ^{31}P NMR spectroscopy. The initial isomerization rates were obtained from linear fits of the initial slopes of plots of the concentration of the products (*cis* and *trans* combined, in mol/L) versus time (min) and normalized to the moles of catalyst used to yield initial turnover frequencies.

The data for each set of catalytic conditions are given in Table 4, and representative examples of the catalytic data for **2**, $\mathbf{2}^+$, and $\mathbf{2}^{2+}$ are shown in Figure 6. Significantly, it was observed that the rate of isomerization was consistently faster for the doubly oxidized form ($\mathbf{2}^{2+}$) than the reduced form (**2**), under identical conditions. Over numerous experiments, it was found that this difference, on average, was 2.2 and 3.3 times faster for the 100:1 and the 10:1 substrate-to-catalyst ratios, respectively. Moreover, the mixed-valence complex ($\mathbf{2}^+$) exhibited an isomerization activity which was identical to the reduced complex (**2**), within experimental error.[22] Therefore, only upon oxidation of the ferrocenyl group on the η^6-arene ligand was a substantial difference in the isomerization activity observed. Although the plots given in Figure 6 are not linear, the data is

Table 4. Catalytic Data for **2**, $\mathbf{2}^+$, and $\mathbf{2}^{2+}$ at 20 °C

catalyst	substrate:catalyst ratio[a]	turnover frequency[b]
2	10:1	0.20 ± 0.07
$\mathbf{2}^{2+}$	10:1	0.66 ± 0.15
2	100:1	0.41 ± 0.06
$\mathbf{2}^+$	100:1	0.39 ± 0.03
$\mathbf{2}^{2+}$	100:1	0.90 ± 0.16

[a] [Substrate] = 1.76 M in CD_2Cl_2 and [catalyst] = 0.176 and 0.0176 M for subtrate to catalyst ratios of 10:1 and 100:1, respectively. [b] Values are an average of two experiments.

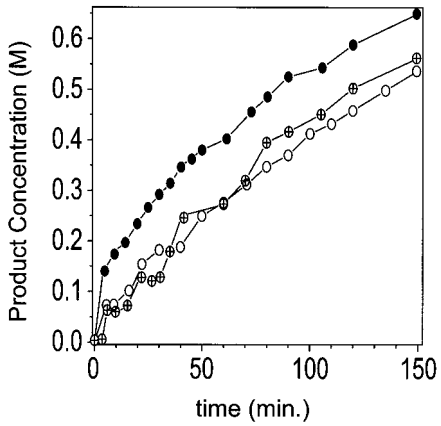

Figure 6. Isomerization studies using a 100:1 substrate to catalyst ratio ([Rh] = 0.017 M and [ethyl allyl ether] = 1.7 M in CD_2Cl_2 at 20 °C) of each oxidation state: (open circle) reduced complex (**2**); (crossed circle) mixed-valance complex ($\mathbf{2}^+$); and (filled circle) doubly oxidized complex ($\mathbf{2}^{2+}$).

(21) (a) Bergens, S. H.; Bosnich, B. *J. Am. Chem. Soc.* **1991**, *113*, 958. (b) Inoue, S.; Takaya, H.; Tani, K.; Otsuka, S.; Sato, T.; Noyori, R. *J. Am. Chem. Soc.* **1990**, *112*, 4897.

very reproducible. It appears that the rate acceleration for the doubly oxidized species occurs at the beginning of the catalytic reaction and then levels off from there on. Perhaps, the product olefin inhibits the reaction. Furthermore, as the reaction proceeded, the activity of all catalysts decreased. This decrease in activity was coincident with the appearance of a doublet in the ^{31}P NMR spectra during the reaction: δ 41.3 (d, J_{Rh-P} = 181.1 Hz). Presumably, this new compound inhibits the isomerization reaction. However, since only the initial rates were studied, where there is no evidence of this doublet or any other additional species, we assume that the differences in the initial rates were not affected by species which appeared at much later reaction times.

Discussion

Compound **2** is an ideal reaction center for studying the effects of RHL oxidation state on complex stoichiometric and catalytic reactivity. In particular, the rates of intramolecular arene−arene exchange can be used as a measure of the relative lability of the weakly coordinating aryl groups in **2**, **2**$^+$, and **2**$^{2+}$. Significantly, it was observed that the exchange rate for **2** substantially increased upon oxidation to **2**$^{2+}$, Table 3. Such arene labilization may be termed the kinetic "RHL effect", and this observed increased arene lability can be understood in two ways. First, it is well-known that decreasing the amount of electron density on a π-ligand by decreasing the number of electron-donating groups decreases the metal−ligand bond strength and, as a result, often increases a π-ligand's lability.[11a,23] Thus, the effect demonstrated herein is similar to previously observed substituent effects; however, with **2** one can electrochemically interconvert an electron-donating ferrocenyl group to an electron-withdrawing ferrocenium group without the use of conventional synthetic steps. Second, it has been shown that arene ligands substituted with strongly electron-donating[24a−c,h,i] or electron-withdrawing substituents[24a−g] can facilitate arene ring slippage through the stabilization of an η^4-intermediate relative to the unsubstituted case. Therefore, since arene−arene exchange reactions commonly involve arene haptotropic shifts,[25,26] those arenes which ease initial ring slippage to an η^4-arene would be expected to display increased lability as compared to benzene. Indeed, there are several examples in which the relative stabilization of an η^4-intermediate is utilized, in part, to explain the increased lability of aromatic ligands with strongly electron-withdrawing or electron-donating substituents when compared to unsubstituted analogs.[24a,f,h,26b,i] In the case of **2**$^{2+}$, the strongly electron-withdrawing ferrocenium group would be expected to facilitate the formation of an η^4-intermediate, such as complex 6 in Scheme 4. This initial ring slippage would be expected to affect the rate of the arene−arene exchange reaction. In related work done in our group, a *cis*-phosphine, *cis*-ether intermediate, such as **7** in Scheme 4, was experimentally determined to be important in the arene−arene exchange process.[12]

Scheme 4

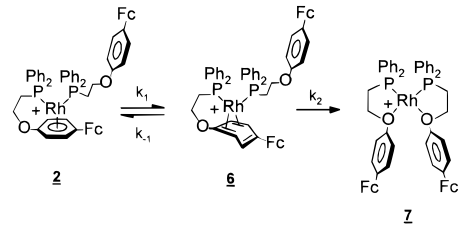

Interestingly, the arene−arene exchange rates for **2** and **2**$^+$ do not differ within experimental error, Table 3 and Figure 4. Since K_{ox}^1 was determined to be 3.8×10^{-3}, the vast majority of complex **2**$^+$ contains a ferrocenylarene bound to the Rh(I) center. Therefore, the similarity in exchange rates for **2** and **2**$^+$ indicate that the displacement of the bound aryl group is important in the intramolecular exchange reaction for all RHL oxidation states; a subsequent fast electron transfer most likely occurs for **2**$^+$ after the rate-determining step.[17] Furthermore, the exchange pathways for **2** and **2**$^+$ likely involve similar mechanisms with a large extent of Rh(I)−arene bond breakage in the transition state as evidenced by their similar large, positive $\Delta H^{\ddagger}$ and $\Delta S^{\ddagger}$ values, Table 3. Such interpretations are reasonable for coordinatively saturated 18-electron complexes, many of which are known to undergo ligand exchange reactions that are dissociative in nature.[25] Moreover, large positive $\Delta H^{\ddagger}$ and $\Delta S^{\ddagger}$ values are suggestive of dissociative pathways, whereas smaller positive $\Delta H^{\ddagger}$ and negative $\Delta S^{\ddagger}$ values reflect associative mechanisms.[25a]

The $\Delta H^{\ddagger}$ value for **2**$^{2+}$ is small as compared with those for **2** and **2**$^+$. This observation is consistent with a decrease in the Rh(I)−arene bond strength accompanying RHL oxidation or alternatively, a significant amount of bond formation accompanying bond breakage in the rate determining step. Also, note the substantial differences in the $\Delta S^{\ddagger}$ values for the doubly oxidized complex (**2**$^{2+}$) as compared to those measured for **2** and **2**$^+$, Table 4. Considering the proposed steps for the arene−arene exchange given in Scheme 4, the differences in the mechanisms for **2** (or **2**$^+$) and **2**$^{2+}$, implied by the two very different $\Delta S^{\ddagger}$ values, can be easily understood. For both **2** and **2**$^+$, the haptotropic shift to yield the η^4-arene ligand (**6**) is not favored, and thus, it is the η^6 to η^4 haptotropic shift which is the slow step in the arene−arene exchange reaction. This breakage of the Rh(I)−arene bond in the transition state is consistent with the large positive $\Delta S^{\ddagger}$ values observed for **2** and **2**$^+$. In contrast, since **2**$^{2+}$ favors arene slippage more than **2** and **2**$^+$, the coordination of the internal ether of the free ferrocenyl−aryl ether is the important step in the reaction. The negative $\Delta S^{\ddagger}$ and the small positive $\Delta H^{\ddagger}$ for the arene−arene exchange reaction involving **2**$^{2+}$ are consistent with Rh(I)−ether bond formation accompanying arene ring slippage in the transition state. Finally, if the differences in the activation parameters for **2**, **2**$^+$, and **2**$^{2+}$ were merely due to different

(22) Only a 100:1 substrate-to-catalyst ratio was used for **2**$^+$. At a 10:1 substrate-to-catalyst ratio, the resonances of the ^{1}H NMR spectra of **2**$^+$ interfere with the accurate integration of both the substrate and product resonances.

(23) (a) Bowyer, W. J.; Merkert, J. W.; Geiger, W. E.; Rheingold, A. L. *Organometallics* **1989**, *8*, 191. (b) Koelle, U.; Fuss, B.; Rajasekharan, M. V.; Ramakrishna, B. L.; Ammeter, J. H.; Böhm, M. C. *J. Am. Chem. Soc.* **1984**, *106*, 4152. (c) Yur'eva, L. P.; Peregudova, S. M.; Nekrasov, L. N.; Korotkov, A. P.; Zaitseva, N. N., Zakurin, N. V.; Vasil'kov, A. Y. *J. Organomet. Chem.* **1981**, *219*, 43. (d) Hamon, J.-R.; Astruc, D.; Michaud, P. *J. Am. Chem. Soc.* **1981**, *103*, 758.

(24) (a) Watts, W. E. in *Comprehensive Organometallic Chemistry*: Wilkinson, G., Ed.; Pergamon: New York, 1982; Vol. 8, p 1050. (b) Hunter, A. D.; Mozol, V.; Tsai, S. D. *Organometallics* **1992**, *11*, 2251. (c) Hunter, A. D.; Shilliday, L.; Furey, W. S.; Zaworotko, M. J. *Organometallics* **1992**, *11*, 1550. (d) Clack, D. W.; Kane-Maguire, L. A. P. *J. Organomet. Chem.* **1978**, *145*, 201. (e) Traylor, T. G.; Hanstein, W.; Berwin, H. J.; Clinton, N. A.; Brown, R. S. *J. Am. Chem. Soc.* **1971**, *93*, 5715. (f) Trahanovsky, W. S.; Wells, D. K. *J. Am. Chem. Soc.* **1969**, *91*, 5870. (g) Wells, D. K.; Trahanovsky, W. S. *J. Am. Chem. Soc.* **1969**, *91*, 5872. (h) Le Maux, P.; Saillard, J. Y.; Granjean, D.; Jaouen, G. *J. Org. Chem.* **1980**, *45*, 4524. (i) Pidcock, A.; Smith, J. D.; Taylor, B. W. *J. Chem. Soc. A* **1969**, 1604.

(25) (a) Howell, J. A. S.; Burkinshaw, P. M. *Chem. Rev.* **1983**, *83*, 557. (b) Kündig, E. P.; Desobry, V.; Grivet, C.; Rudolph, B.; Spichiger, S. *Organometallics* **1987**, *6*, 1173. (c) Howell, J. A. S.; Dixon, D. T.; Kola, J. C.; Ashford, N. F. *J. Organomet. Chem.* **1985**, *294*, C1. (d) Muetterties, E. L.; Bleeke, J. R.; Sievert, A. C. *J. Organomet. Chem.* **1979**, *178*, 197.

(26) (a) Traylor, T. G.; Goldberg, M. J. *J. Am. Chem. Soc.* **1987**, *109*, 3968. (b) Traylor, T. G.; Stewart, K. J.; Goldberg, M. J. *J. Am. Chem. Soc.* **1984**, *106*, 4445. (c) Pidcock, A.; Smith, J. D.; Taylor, B. W. *J. Chem. Soc. A* **1967**, 872. (d) Zingales, F.; Chiesa, A.; Basolo, F. *J. Am. Chem. Soc.* **1966**, *88*, 2707.

solvation of the charged transition states, then the measured $\Delta S^{\ddagger}$ for the mixed-valence form ($\mathbf{2}^{+}$) should differ significantly from that for **2**, but it does not.

The first reactivity consequence of the increased lability of the Rh(I)−arene bond upon oxidation of the chelated ligand was observed by studying complex **2** and its charge-dependent interactions with CH_3CN. From a comparison of the cyclic voltammetry data of **2** in the absence and presence of 1% CH_3CN in CH_2Cl_2, a 100-fold increase in its CH_3CN bonding affinity was observed upon moving from its totally reduced to totally oxidized state ($\mathbf{2}^{2+}$). These oxidation-state-dependent equilibria can be viewed as a measure of the thermodynamic "RHL effect". Note that this reactivity pattern is consistent with the 3.3 kcal/mol destabilization of **2** that accompanies double oxidation to form $\mathbf{2}^{2+}$.

Numerous η^6-arene transition metal complexes are catalytically active.[27,28] In some cases, the arene ligand stays bound to the metal center throughout the reaction cycle.[27b,c] Of more interest to us, however, are cases in which the arene ligand is substitutionally labile on the metal center and acts to stabilize the complex in the absence of substrate or coordinating solvent.[28] For several such complexes, it was shown that initial arene displacement[28a−c] or ring slippage[28d−f] was essential for the occurrence of reactions at the bound transition metal center. Furthermore, it has been observed that too strong of a metal−arene bond can result in complete deactivation of a reactive metal catalyst.[29] Since the EXSY data given in Table 3 are consistent with arene labilization in $\mathbf{2}^{2+}$, the lability of the η^6-aryl group in **2**, $\mathbf{2}^{+}$, and $\mathbf{2}^{2+}$ was expected to have an effect on complex catalytic activity. To test this, a catalytic reaction was chosen where the initial displacement of the arene moiety and an opening of coordination sites at the metal center were important steps in the reaction cycle.

The isomerization activity studies of **2**, $\mathbf{2}^{+}$, and $\mathbf{2}^{2+}$ performed herein demonstrate for the first time that the catalytic activity of an RHL complex can be significantly altered upon ligand oxidation. Note that the doubly oxidized complex ($\mathbf{2}^{2+}$) exhibits a significant increase in its catalytic activity upon ligand oxidation when compared to the reduced (**2**) or the mixed-valence ($\mathbf{2}^{+}$) forms, Table 4. This observation is consistent with the proposed decrease in the Rh(I)−arene-bonding interaction that accompanies oxidation of $\mathbf{2}^{+}$ to $\mathbf{2}^{2+}$. Furthermore, this observation suggests that η^6-arene displacement or ring slippage in the starting 18-electron complex is an important step in the catalytic cycle. In addition, the observation that the isomerization activity of $\mathbf{2}^{+}$ does not differ from that of **2** is extremely important. This confirms that the lability of the bound η^6-arene moiety in **2**, $\mathbf{2}^{+}$, and $\mathbf{2}^{2+}$ is the major factor in this system that controls isomerization rates. It is unlikely that these oxidation-state-dependent activities are merely due to differences in complex charge or solvation. In that case, one would expect significant differences in the activities for **2** and $\mathbf{2}^{+}$.

Conclusions

Redox-switchable hemilabile ligands (RHLs), such as **1**, offer tremendous control over both the steric and electronic environments of bound transition metal centers and, thus, metal complex reactivity. The Rh(I)−RHL complex (**2**) has provided a novel system for the facile investigation of both the kinetic and thermodynamic effects associated with complex oxidation. With **2**, we have shown that ligand oxidation not only accelerates an intramolecular exchange reaction, but also changes the mechanism through which such a reaction occurs. Furthermore, we have demonstrated that RHLs can be utilized to modulate transition metal complex reactivity via the selective and electrochemically induced opening and closing of coordination sites at a reactive transition metal center. When optimized, such systems may be useful for catalyst storage and activation and, therefore, the easy use and recovery of expensive homogeneous transition metal catalysts. Presently, we are improving the RHL design in an effort to understand fundamental factors that will yield the maximum oxidation-state-dependent effects on complex reactivity.

Experimental Section

General. All reactions were carried out under nitrogen using standard Schlenk techniques or in an inert atmosphere glovebox unless noted otherwise. All solvents were treated as previously described.[4a,12] Ferrocenylphenol[9] and $[RhCl(COT)_2]_2$[10] were prepared according to literature procedures. $RhCl_3 \cdot xH_2O$ was used on loan from Johnson-Matthey Chemical Co. Ethyl allyl ether was purchased from Aldrich Chemical Co. and distilled over K_2CO_3 and degassed prior to use. All other chemicals were purchased from Aldrich Chemical Co. and used as received.

Physical Measurements. One-dimensional ^1H NMR spectra were recorded on either a Varian Gemini 300 MHz or a Varian Unity 400 MHz FT-NMR spectrometer. $^{31}P\{^1H\}$ NMR spectra were recorded on either a Varian Gemini 300 MHz or a Varian Unity 400 MHz FT-NMR spectrometer at 121 and 162 Hz, respectively, and referenced versus the external standard of 85% H_3PO_4. 2D ^1H NMR COSY experiments were performed on a Varian Unity 400 MHz FT-NMR spectrometer. ^1H NMR exchange spectroscopy (EXSY) spectra were recorded on a Varian Unity 400 MHz FT-NMR spectrometer using a standard NOESY pulse sequence with t_m varying with temperature. Electrochemical measurements were carried out on a PINE AFRDE4 or AFRDE5 bipotentiostat using a glassy carbon working electrode (8.0×10^{-5} cm^2), a Pt mesh counter electrode, and a Ag wire reference electrode. In all cases a 0.1 M solution of $^nBu_4NPF_6$ was used as the supporting electrolyte. All electrochemical data are referenced versus the FcH/FcH^+ [$Fc = (\eta^5\text{-}C_5H_5)Fe(\eta^5\text{-}C_5H_4)$] redox couple. Electron ionization (EI) and fast atom bombardment (FAB) mass spectra were recorded on a Fisions VG 70-250 SE mass spectrometer. Elemental analyses were done by either Desert Analytics, Tucson, AZ, or Schwarzkopf Microanalytical Laboratory Inc., Woodside, NY.

Synthesis of $(\eta^5\text{-}C_5H_5)Fe(\eta^5\text{-}C_5H_4C_6H_4OCH_2CH_2Cl)$. Ferrocenylphenol[9] (2.92 g, 0.011 mol), KOH (1.20 g, 0.023 mol), dichloroethane (41.4 mL, 0.525 mol), and a catalytic amount of the phase transfer catalyst *n*-Bu_4NI were refluxed with 150 mL of distilled water in air. After 15 h, 150 mL of distilled water and 150 mL of CH_2Cl_2 were added to the crude reaction mixture. The organic phase was separated, washed once with distilled water, and dried over $MgSO_4$. Column chromatography of the crude product on silica gel was performed. Starting material was eluted with 100% pentane and a second band was eluted by increasing the percentage of CH_2Cl_2 until a 100% CH_2Cl_2 eluent was obtained. This band was concentrated by vacuum evaporation of the solvent to yield an analytically pure orange microcrystalline sample of **$(\eta^5\text{-}C_5H_5)Fe(\eta^5\text{-}C_5H_4C_6H_4OCH_2CH_2Cl)$, (yield = 46%, 1.73 g, 0.051 mol).** **^1H NMR** ($CDCl_3$): δ 3.81 (t, J_{H-H} = 5.93 Hz, 2H, CH_2Cl), 4.01 (s, 5H, η^5-C_5H_5), 4.22 (t, J_{H-H} = 5.94

(27) (a) Muetterties, E. L.; Bleeke, J. R. *Acc. Chem. Res.* **1979**, *12*, 324. (b) Amaratunga, S.; Alper, H. *J. Organomet. Chem.* **1995**, *488*, 25. (c) Amer, I.; Alper, H. *J. Am. Chem. Soc.* **1990**, *112*, 3674. (d) Davies, S. G.; Green, M. L. H.; Mingos, D. M. P. *Tetrahedron* **1978**, *34*, 3047. (e) Tsonis, C. P.; Farona, M. F. *J. Organomet. Chem.* **1976**, *114*, 293. (f) White, J. F.; Farona, M. F. *J. Organomet. Chem.* **1973**, *63*, 329.

(28) (a) Bönnemann, H.; Goddard, R.; Grub, J.; Mynott, R.; Raabe, E.; Wendel, S. *Organometallics* **1989**, *8*, 1941. (b) Fairlie, D. P.; Bosnich, B. *Organometallics* **1988**, *7*, 936. (c) Klabunde, K. J.; Anderson, B. B.; Bader, M.; Radonovich, L. J. *J. Am. Chem. Soc.* **1978**, *100*, 1313. (d) Choe, S.-B.; Kanai, H.; Klabunde, K. J. *J. Am. Chem. Soc.* **1989**, *111*, 2875. (e) Johnson, J. W.; Muetterties, E. L. *J. Am. Chem. Soc.* **1977**, *99*, 7395. (f) Shmidt, F. K.; Levkovskii, Y. S.; Saraev, V. V.; Ryutina, N. M.; Kosinskii, O. L.; Bukunina, T. I. *React. Kinet. Catal. Lett.* **1977**, *7*, 445.

(29) (a) Nickel, T.; Goddard, R.; Krüger, C.; Pörschke, K.-R. *Angew. Chem., Int. Ed. Engl.* **1994**, *33*, 879. (b) Fish, R. H.; Kim, H.-S.; Babin, J. E.; Adams, R. D. *Organometallics* **1988**, *7*, 2250. (c) Crabtree, R. H.; Mellea, M. F.; Quirk, J. M. *J. Am. Chem. Soc.* **1984**, *106*, 2913. (d) Lucherini, A.; Porri, L. *J. Organomet. Chem.* **1978**, *155*, C45.

Hz, 2H, OCH_2), 4.25 (t, J_{H-H} = 1.80 Hz, 2H, η^5-C_5H_4), 4.55 (t, J_{H-H} = 1.71 Hz, 2H, η^5-C_5H_4), 6.84 (m, 2H, C_6H_4), 7.39 (m, 2H, C_6H_4). MS (EI): M^+ = 340 *m/z*. Anal. ($C_{18}H_{17}ClFeO$) C, calcd 63.47, found 63.47; H, calcd 5.03, found 4.83.

Synthesis of (η^5-C_5H_5)Fe(η^5-$C_5H_4C_6H_4OCH_2CH_2PPh_2$) (1). A THF solution of $KPPh_2$ (0.50 M, 1.11 mmol) was added slowly to a solution of (η^5-C_5H_5)Fe(η^5-$C_5H_4C_6H_4OCH_2CH_2Cl$) (0.361 g, 1.05 mmol) in 70 mL of THF at 0 °C. The reaction mixture was allowed to warm to room temperature over 12 h, and the solution was concentrated to dryness in vacuo. A CH_2Cl_2 solution of the crude reaction mixture was added to a flask equipped with 20 g of silica gel, leaving the KCl behind, and the solvent was removed in vacuo. Column chromatography of the crude product was performed in a glovebox under nitrogen. Three bands were eluted with a 1:1 pentane to CH_2Cl_2 solution. The first band contained mostly $HPPh_2$ and was discarded. The second band contained mostly starting material and was saved. The third and major band contained **1**. Vacuum evaporation of the solvent afforded the desired ligand **1** as a yellow microcrystalline solid (yield = 80%, 414 mg, 0.85 mmol). ^{1}H NMR ($CDCl_3$): δ 2.62 (t, J_{H-H} = 7.55 Hz, 2H, CH_2PPh_2), 4.00 (s, 5H η^5-C_5H_5), 4.09 (q, J_{H-H} = 7.62 Hz, 2H, CH_2O), 4.23 (t, J_{H-H} = 1.83 Hz, 2H, η^5-C_5H_4), 4.53 (t, J_{H-H} = 1.86 Hz, 2H, η^5-C_5H_4), 6.71 (m, 2H, C_6H_4), 7.34 (m, 4H, C_6H_4 and PPh_2), 7.48 (m, 8H, PPh_2). ^{31}P NMR ($CDCl_3$): δ −22.2 (s); FAB-HRMS: M^+ calcd 490.1149, found 490.1123 *m/z*. Anal. ($C_{30}H_{27}FeOP$): C, calcd 73.48, found 73.16; H, calcd 5.55, found 5.18. $E_{1/2}$ = −27 mV vs FcH/FcH^+ (CH_2Cl_2/0.1 M $^nBu_4NPF_6$).

Synthesis of [(η^1:η^6-(η^5-C_5H_5)Fe(η^5-$C_5H_4C_6H_4OCH_2CH_2PPh_2$))-($\eta^1$-($\eta^5$-$C_5H_5$)Fe($\eta^5$-$C_5H_4C_6H_4OCH_2CH_2PPh_2$))Rh]$^+$$BF_4^-$ (2). [RhCl(COT)$_2$]$_2$[10] (40.2 mg, 0.112 mmol) and $AgBF_4$ (22.7 mg, 0.116 mmol) were reacted in 4 mL of CH_2Cl_2 for 50 min. The resulting reaction mixture was filtered over Celite to remove a light gray precipitate and diluted with 300 mL of CH_2Cl_2. A solution of 1 (110.0 mg, 0.224 mmol) in 150 mL of CH_2Cl_2 was added dropwise at −78 °C. After 3.5 h, the solvent was removed in vacuo to yield a red-orange powder. Pure samples of **2** were obtained by layering a CH_2Cl_2 solution of the product with diethyl ether three to six times (yield = 45%, 120 mg, 0.050 mmol). ^{1}H NMR (CD_2Cl_2): δ 1.71 (q, 2H, CH_2PPh_2 chelated), 2.06 (m, 2H, CH_2PPh_2 free), 3.80−4.02 (m, 7H, CH_2O chelated and η^5-C_5H_5 free), 4.06 (s, 5H, η^5-C_5H_5 chelated), 4.14 (m, 2H, CH_2O free), 4.20 (m, 2H, η^5-C_5H_4), 4.23 (m, 2H, η^5-C_5H_4), 4.34 (m, 2H, η^5-C_5H_4), 4.65 (m, 2H, η^5-C_5H_4), 6.66 (m, 2H, C_6H_4 free), 6.86 (m, 4H, η^6-C_6H_4), 7.12 (m, 8H, PPh_2), 7.25−7.48 (m, 14H, C_6H_4 free and PPh_2). ^{31}P NMR (CD_2Cl_2): δ 34.9 (dd, J_{Rh-P} = 204.4 Hz, J_{P-P} = 39.3 Hz), 31.3 (dd, J_{Rh-P} = 209.7 Hz, J_{P-P} = 39.3 Hz). FAB-HRMS: M^+ calcd 1083.1353, found 1083.1313 *m/z*.

Synthesis of [(η^1:η^6-(η^5-C_5H_5)Fe(η^5-$C_5H_4C_6H_4OCH_2CH_2PPh_2$))-($\eta^1$-($\eta^5$-$C_5H_5$)Fe($\eta^5$-$C_5H_4C_6H_4OCH_2CH_2PPh_2$))Rh]$^{2+}$($BF_4^-$)$_2$ (2^{2+}). 2 (18 mg, 0.0154 mmol) and 1 equiv of $AgBF_4$ (3 mg, 0.0154 mmol) were reacted in 1.0 mL of CD_2Cl_2. After 1 min, an Ag^0 mirror was observed and a dark burgundy red solution was collected upon filtration over Celite. Once the oxidation reaction was shown to be complete by NMR (spectroscopic yield >98%), the sample was used for kinetic NMR and reactivity studies. ^{1}H NMR (CH_2Cl_2): δ 0.95 (q, J_{H-H} = 7.65 Hz, 2H, CH_2PPh_2 chelated), 1.79 (m, 2H, CH_2PPh_2 free), 3.79 (m, 2H, CH_2O chelated), 3.81 (m, 2H, η^5-C_5H_4), 3.89 (m, 2H, η^5-C_5H_4), 3.95 (dt, J_{P-H} = 21.0 Hz, J_{H-H} = 4.40 Hz, CH_2O free), 4.10 (s, 5H, η^5-C_5H_5), 4.56 (b, ferrocenium), 6.38 (m, 4H, C_6H_4), 6.69 (m, 4H, η^6-C_6H_4), 6.81−7.31 (m, 20H, PPh_2), 8.62 (b, ferrocenium), 11.0 (b, ferrocenium). ^{31}P NMR (CH_2Cl_2): δ 34.3 (dd, J_{Rh-P} = 203.9 Hz, J_{P-P} = 39.5 Hz), 30.3 (dd, J_{Rh-P} = 210.7 Hz, J_{P-P} = 39.5 Hz).

Synthesis of [(η^1:η^6-(η^5-C_5H_5)Fe(η^5-$C_5H_4C_6H_4OCH_2CH_2PPh_2$))-($\eta^1$-($\eta^5$-$C_5H_5$)Fe($\eta^5$-$C_5H_4C_6H_4OCH_2CH_2PPh_2$))Rh]$^{3+}$($BF_4^-$)$_3$ (2^{2+}). 2 (18 mg, 0.0154 mmol) and 2 equiv of $AgBF_4$ (6 mg, 0.0308 mmol) were reacted in 1.0 mL of CD_2Cl_2. After 1 min, a Ag^0 mirror was observed and a very dark burgundy red solution was collected upon filtration over Celite. Once the oxidation reaction was shown to be complete by NMR (spectroscopic yield >98%), the sample was used for kinetic NMR and reactivity studies. ^{1}H NMR (CH_2Cl_2): δ −6.28 (b, ferrocenium), −3.61 (b, ferrocenium), 0.27 (q, J_{H-H} = 7.52 Hz, 2H, CH_2PPh_2 chelated), 1.53 (m, 2H, CH_2PPh_2 free), 2.58 (b, ferrocenium), 3.67 (m, 2H, CH_2O chelated), 3.52 (b, ferrocenium), 3.79 (m, 2H, CH_2O free), 4.32 (m, 4H, C_6H_4), 5.85 (m, 4H, η^6-C_6H_4), 6.30−7.13 (m, 20H, PPh_2), 14.85 (b, ferrocenium), 17.18 (b, ferrocenium). ^{31}P NMR (CH_2Cl_2): δ 33.4 (dd, J_{Rh-P} = 203.0 Hz, J_{P-P} = 39.4 Hz), 29.0 (dd, J_{Rh-P} = 210.3 Hz, J_{P-P} = 39.4 Hz).

Reaction of 2 with Acetonitrile. In an NMR tube, complex **2** was reacted with neat CD_3CN to form a mixture of *cis*- and *trans*-bis(acetonitrile) adducts, [*cis*-(η^1-(η^5-C_5H_5)Fe(η^5-$C_5H_4C_6H_4OCH_2CH_2PPh_2$))$_2$($CH_3CN$)$_2$Rh]$^+$$BF_4^-$ (**4**) and [*cis*-(η^1-(η^5-C_5H_5)Fe(η^5-$C_5H_4C_6H_4OCH_2CH_2PPh_2$))$_2$($CH_3CN$)$_2$Rh]$^+$$BF_4^-$ (**5**), in a 3:1 ratio, respectively. Upon removal of the CD_3CN by exposure to vacuum for 48 h, only the arene-coordinated product (**2**) was observed. In CD_2Cl_2 with **2** equiv of CH_3CN a similar mixture of **4** and **5** is formed. If this reaction is performed at −78 °C, only the cis adduct (**4**) forms. As the temperature is raised to 25 °C, the *cis* adduct slowly converts to the trans adduct until a ratio of 3:1 is reached. Data for **4**. ^{1}H NMR (CH_2Cl_2, −78 °C): δ 1.62 (s, 6H, CH_3CN), 2.07 (m, 4H, CH_2PPh_2), 3.98 (s, 10H, η^5-C_5H_5), 4.43 (m, 4H, CH_2O), 4.32 (m, 4H, η^5-C_5H_4), 4.60 (m, 4H, η^5-C_5H_4), 6.69 (d, J_{H-H} = 6.3 Hz, 4H, C_6H_4), 7.23−7.38 (m, 24H, C_6H_4 and PPh_2). ^{31}P NMR (CH_2Cl_2): δ 35.9 (d, J_{Rh-P} = 174.8 Hz). Data for **5**. ^{1}H NMR (CH_2Cl_2, 25 °C): δ 1.94 (s, 6H, CH_3CN), 2.23 (m, 4H, CH_2PPh_2), 4.01 (s, 10H, η^5-C_5H_5), 4.27 (m, 4H, η^5-C_5H_4), 4.41 (m, 4H, CH_2O), 4.57 (m, 4H, η^5-C_5H_4), 6.64 (d, J_{H-H} = 8.0 Hz, 4H, C_6H_4), 7.29−7.55 (m, 24H, C_6H_4 and PPh_2). ^{31}P NMR (CH_2Cl_2): δ 22.2 (d, J_{Rh-P} = 131.7 Hz).

NMR Kinetic Studies. 2D exchange spectroscopy (EXSY) was used to determine the rates and activation parameters of the arene-arene exchange reactions of **2**, $\mathbf{2}^+$, and $\mathbf{2}^{2+}$. A standard 2D NOESY pulse sequence (d_1 (relaxation) − $\pi/2$ − t_1 − $\pi/2$ − t_m (mixing) − $\pi/2$ − t_2 (aquisition)) was used on a Varian 400 MHz FT NMR spectrometer. The region of the ^{1}H NMR spectrum which contained the CH_2PPh_2 resonances was used to measure rate data since those resonances were well resolved for all oxidation states of **2**. Mixing times (t_m) were varied with temperature. The rate of the exchange reaction was determined by comparing the volumes of the cross peaks (V_{AB} and V_{BA}) and the diagonal peaks (V_{AA} and V_{BB}) and evaluating the mixing time in the equation $k = 1/t_m \ln[(r+1)/(r-1)]$, where $r = (V_{AA} + V_{BB})/(V_{AB} + V_{BA})$.[16] From a plot of $\ln(k/T)$ versus $1/T$ modeled according to the Eyring equation, $\Delta H^‡$ and $\Delta S^‡$ values for the exchange reaction were calculated.[18] Using the Eyring equation in the form $\Delta G^‡ = -RT \ln(hk/k_bT\kappa)$, where κ is 0.5, $\Delta G^‡_{(293)}$ values were calculated. These values agreed well with those obtained using $\Delta H^‡$ and $\Delta S^‡$ in the equation $\Delta G^‡ = \Delta H^‡ - T\Delta S^‡$. To confirm these data, each point on the Eyring plot was measured in two to four separate experiments. From these data, errors in the exchange rates (Δk) were estimated for **2**, $\mathbf{2}^+$, and $\mathbf{2}^{2+}$. Using a CD_3OD ^{1}H NMR standard, the average fluctuation in the probe temperature from the desired values (ΔT) was determined to be ±0.5 °C. Errors in $\Delta G^‡$ were obtained by applying Δk and ΔT to the Eyring equation.[18] The analysis of errors in $\Delta H^‡$ and $\Delta S^‡$ was performed by fitting all plots of $\ln(k/T)$ vs $1/T$ to give the minimum and maximum slopes. These slopes, and the resulting *y*-intercept values, were used to calculate the minimum and maximum values of $\Delta H^‡$ and $\Delta S^‡$, respectively. The largest differences from the best fit of the experimental data were taken as generous estimates of the errors in $\Delta H^‡$ and $\Delta S^‡$.

Isomerization Studies of 2, 2^+, and 2^{2+}. In a 5-mm diameter NMR tube equipped with an air-free screw cap top and Teflon septa was placed either **2** (0.010 mmol), $\mathbf{2}^+$ (0.010 mmol), or $\mathbf{2}^{2+}$ (0.010 mmol) in 0.48 mL of CD_2Cl_2. To the catalyst solution was added 0.12 mL of ethyl allyl ether via an air-free syringe. The tube was then vigorously shaken for 30 s and then placed into the probe at 20 °C. The progress of the reaction was monitored by ^{1}H NMR, and the Rh catalyst was monitored by ^{31}P NMR spectroscopy. Initial rates of isomerization were obtained by plotting product concentration (*cis* and *trans* combined) versus time. The best fit of the initial slope of these data was taken as the initial rate, and all rates were normalized for the moles of catalyst present to give the initial turnover frequencies. Each catalytic run was performed at least two times to confirm the results.

Crystallographic Structure Determination. Single crystals of **2**·1.25CH_2Cl_2 suitable for the X-ray diffraction study were grown by the slow diffusion of pentane into a CH_2Cl_2 solution of **2**. Crystal, data collection, and refinement parameters are given in Table 1. The systematic absences in the diffraction data were consistent for the space groups $P1$ and $P\bar{1}$. The *E*-statistics strongly suggested the centrosym-

metric space group $P\bar{1}$ that yielded chemically reasonable and computionally stable results of refinement. The structure was solved by direct methods, completed by a subsequent difference Fourier syntheses, and refined by a full-matrix least-squares procedures. Two independently but chemically equivalent ion pairs were located in the asymmetric unit. Also, there were 2.5 solvate molecules of methylene chloride in the asymmetric unit. All non-hydrogen atoms were refined with anisotropic displacement coefficients. One of the solvate molecules was disordered over an inversion center. One chlorine atom in the disordered solvent molecule was furthered disordered between two positions, 70:30, and was refined isotropically, and the hydrogen atoms in the molecule were ignored due to disorder. Hydrogen atoms were treated as idealized contributions.[30] No attempt to locate the hydrogen atom on the disordered solvent molecule was made. Supporting Information contains further details of the structure determination.

(30) All software and sources of scattering factors are contained in the SHELXTL (version 5.03) program library (G. Sheldrick, Siemens XRD, Madision, WI).

Acknowledgment. We acknowledge the NSF (CHE-9625391 and CHE-9357099) and the Petroleum Research Fund (No. 30759-AC3) for generously funding this research. C.A.M. also acknowledges an A. P. Sloan Foundation Fellowship and a Camille Dreyfus Teacher−Scholar Award. C.S.S. acknowledges an ARCS Foundation Fellowship.

Supporting Information Available: A detailed description of the X-ray diffraction study of **2**·1.25CH_2Cl_2, including tables of experimental details, atom positional parameters, *B*(eq) values, bond lengths, bond angles, and anisotropic displacement parameters (17 pages). See any current masthead page for ordering and Internet access instructions.

JA9723601